Proteins of nucleotide and base excision repair pathways interact in mitochondria to protect from loss of subcutaneous fat, a hallmark of aging

York Kamenisch,[1] Maria Fousteri,[3] Jennifer Knoch,[1]
Anna-Katharina von Thaler,[1] Birgit Fehrenbacher,[1] Hiroki Kato,[2]
Thomas Becker,[4] Martijn E.T. Dollé,[5] Raoul Kuiper,[5] Marc Majora,[6]
Martin Schaller,[1] Gijsbertus T.J. van der Horst,[7] Harry van Steeg,[5]
Martin Röcken,[1] Doron Rapaport,[2] Jean Krutmann,[6] Leon H. Mullenders,[3]
and Mark Berneburg[1]

[1]Department of Dermatology and [2]Interfaculty Institute for Biochemistry, Eberhard Karls University, D-72076
Tuebingen, Germany
[3]Department of Toxicogenetics, Leiden University Medical Center, 2300 RC Leiden, Netherlands
[4]Institut für Biochemie und Molekularbiologie, ZBMZ, Universität Freiburg, 79104 Freiburg, Germany
[5]Health Protection Research, National Institute of Public Health and the Environment, Pathobiology Department, Dutch
 Molecular Pathology Centre, Utrecht University, 3508 TD Utrecht, Netherlands
[6]Institut für Umweltmedizinische Forschung IUF, D-40225 Düsseldorf, Germany
[7]Department of Genetics, Erasmus University Medical Center, 3015 GE Rotterdam, Netherlands

Defects in the DNA repair mechanism nucleotide excision repair (NER) may lead to tumors in xeroderma pigmentosum (XP) or to premature aging with loss of subcutaneous fat in Cockayne syndrome (CS). Mutations of mitochondrial (mt)DNA play a role in aging, but a link between the NER–associated CS proteins and base excision repair (BER)–associated proteins in mitochondrial aging remains enigmatic. We show functional increase of CSA and CSB inside mt and complex formation with mtDNA, mt human 8-oxoguanine glyco-sylase (mtOGG)-1, and mt single-stranded DNA binding protein (mtSSBP)-1 upon oxidative stress. MtDNA mutations are highly increased in cells from CS patients and in subcutaneous fat of aged $Csb^{m/m}$ and $Csa^{-/-}$ mice. Thus, the NER–proteins CSA and CSB localize to mt and directly interact with BER–associated human mitochondrial 8-oxoguanine glycosylase–1 to protect from aging– and stress–induced mtDNA mutations and apoptosis–mediated loss of subcutaneous fat, a hallmark of aging found in animal models, human progeroid syndromes like CS and in normal human aging.

CORRESPONDENCE
Mark Berneburg:
mark.berneburg@
med.uni-tuebingen.de

Abbreviations used: 8-oxoG, 7,8-dihydro-8-oxoguanine; BER, base excision repair; CoIP, co-immunoprecipitation; CS, Cockayne syndrome; GEMSA, gel electrophoresis mobility shift assay; mt, mitochondria; mtOGG-1, human mitochondrial 8-oxoguanine glycosylase-1; mtSSBP, mt single-stranded DNA binding protein; NER, nucleotide excision repair; ROS, reactive oxygen species; TCR, transcription-coupled repair; TTD, trichothiodystrophy; XP, xeroderma pigmentosum.

Nucleotide excision repair (NER) is a highly conserved mechanism, responsible for the re-pair of bulky, helix distorting DNA damage induced by UV radiation, cis-platinum, and oxidative stress (Wood, 1989; Lehmann, 1995; Berneburg and Lehmann, 2001; Riedl et al., 2003; van der Wees et al., 2007). Defects in NER can lead to three clinically distinct dis-eases. Xeroderma pigmentosum (XP) results in sun sensitivity, pigmentary changes, and a 2,000-fold increase in skin cancer risk (van

Steeg and Kraemer, 1999). Patients suffering from trichothiodystrophy (TTD) and Cock-ayne syndrome (CS) display growth and mental retardation and sun sensitivity, but not an in-creased skin cancer risk. In addition, CS promotes segmental progeria with growth retardation, hal-onated eyes, and, as a clinical hallmark, reduced subcutaneous fat. CS is caused by mutations in the CSA and CSB genes and cells from these

The Journal of Experimental Medicine

patients are defective in the NER subpathway transcription-coupled (TC)–NER (Nance and Berry, 1992; Furuta et al., 2002; van der Horst et al., 2002; van Hoffen et al., 2003). Previous work demonstrated deficient removal of oxidatively damaged nuclear and mitochondrial DNA in CSB cells (LeDoux et al., 1992; Balajee et al., 1999; Tuo et al., 2001). For the nucleus, recent work could show different roles for repair of UV-induced DNA damage and oxidative stress (Nardo et al., 2009), and interaction of CSB with NEIL-1 (Muftuoglu et al., 2009). Mitochondrial localization has remained enigmatic up to now, which is why it has been hypothesized that functions outside mt may account for repair of oxidative stress in mt (Stevnsner et al., 2008). In addition, the exact molecular function of CSB, and particularly CSA, in response to oxidative stress are unresolved, and mitochondrial localization of CSA and CSB may still be possible. Furthermore, it has been shown that mt are highly efficient in repairing oxidative damage of mtDNA and that they do contain proteins involved in base excision repair (BER), such as human mitochondrial 8-oxo-guanosine glycosylase (mtOGG)-1 (Nishioka et al., 1999; de Souza-Pinto et al., 2001). We investigated whether CSA and CSB (a) are recruited to mt; (b) directly interact with mtDNA and BER-associated human mitochondrial 8-oxoguanine glycosylase-1 (mtOGG-1); (c) are involved in protection from oxidatively induced and aging-associated mtDNA mutations; or (d) lead to the age-associated reduction of subcutaneous fat tissue in $Csa^{-/-}$ and $Csb^{m/m}$ mice.

RESULTS

Recruitment of CSA and CSB proteins to mt in response to oxidative stress

We started by asking whether the CSA and CSB proteins, known to be present predominantly in the nucleus, are also localized in mt. Immunocytostaining with antibodies against CSA or CSB and against mitochondrial marker proteins, as well as nuclear staining with subsequent confocal laser scanning microscopy, was performed in normal and CSA- and CSB-deficient fibroblasts (see Tables S1, S3, and S4 for detailed cell lines and antibodies). In normal fibroblasts, CSA (Fig. 1 A) and CSB (Fig. 1 B), proteins were virtually undetectable in mt; however, these proteins were clearly visible in the nucleus with some minor localization at the cytoplasm (Fig. 1, A and B). Confocal images of cells without nuclear staining confirmed the presence of CSA and CSB proteins in the nucleus and cytoplasm (Fig. S1 and not depicted). Confocal microscopy of CSA and CSB cells with the CSA and CSB antibodies, respectively, validated the specificity of the antibodies (Fig. 1, A and B, and Fig. S1). Note that in the absence of a functional CSB protein (CSB cells; Fig. 1 A, bottom), an increased cytoplasmic staining of CSA was observed, whereas the nuclear staining was similar in both CSB and normal cells.

Genotoxic stress is known to increase CSA localization to the sites of nuclear DNA damage (Kamiuchi et al.,

2002). To determine whether oxidative stress is capable of inducing the CSA and CSB protein levels in mt, we exposed human CSA- and CSB-deficient and normal fibroblasts to 25 μM H_2O_2 for 12 h. This treatment did not affect cellular viability. In contrast to the unstressed situation, CSA (Fig. 1 C) and CSB (Fig. 1 D) proteins were clearly detectable by confocal microscopy in mt after oxidative stress. The staining was highly specific, as the CSA or CSB proteins were undetectable in mt or nuclei of cells defective in CSA or CSB, respectively. CSA and CSB cells complemented with the respective hemagglutinin (HA)-tagged-WT CSA and HA-tagged-WT CSB proteins showed reconstitution of CSA (Fig. 1 E) and CSB (not depicted) in mt to WT levels. Confocal microscopy of cells without nuclear staining showed the presence of CSA (Fig. S2) protein in the nucleus and mt. Similar results were obtained when cells were exposed to a UVA-induced oxidative stress as reported previously (Berneburg et al., 1999, 2004, 2005; Lin and Beal, 2006) instead of H_2O_2 (unpublished data).

To confirm results at the molecular level and to quantify the amount of each protein in the different cell compartments, whole-cell and mitochondrial extracts were isolated from oxidatively stressed cells and subsequently analyzed by PCR and Western blotting. PCR revealed the absence of nuclear GAPDH-DNA in mitochondrial extracts (Fig. 1 F), whereas PCR using previously published mitochondrial primers (Berneburg et al., 1999, 2004, 2005; Lin and Beal, 2006) showed a strong signal for the presence of mtDNA (IS; Fig. 1 F). This was confirmed at the protein level by the presence of mitochondrial ATP-synthase in all extracts (Fig. 1 F) and the absence of nuclear phosphorylated NF-κB in mitochondrial extracts, but its presence in whole-cell extracts (Fig. 1 F). Immunoblot analysis of mitochondrial extracts for S6 ribosomal protein also revealed lack of this protein in mitochondrial extracts verifying the absence of cytoplasmic contamination (Fig. 1 F). Nevertheless, immunoblot analysis of stressed cells revealed the presence of CSA and CSB proteins in both whole-cell and mitochondrial extracts of normal cells, whereas CS-deficient cells remained negative (Fig. 1 F).

As the presence of the nuclear CSA and CSB proteins in mt has not been reported before, we used immunoelectron-microscopy as a third method to verify our findings. Gold-labeled antibodies against CSA or CSB clearly demonstrated the localization of both proteins in oxidatively stressed mt (circles; Fig. 1 G).

To further demonstrate the location of CSA and CSB within the organelle, protease protection assays were performed (Fig. 1 H). CSA (Fig. 1 H, top) and CSB (Fig. 1 H, bottom) proteins in oxidatively stressed mt are protected from proteinase K digestion. However, disintegration of mitochondrial membranes by Triton X-100 renders CSA and CSB proteins sensitive to proteinase K digestion. These results show that CSA is located within mt and exclude unspecific association at the surface of the organelle.
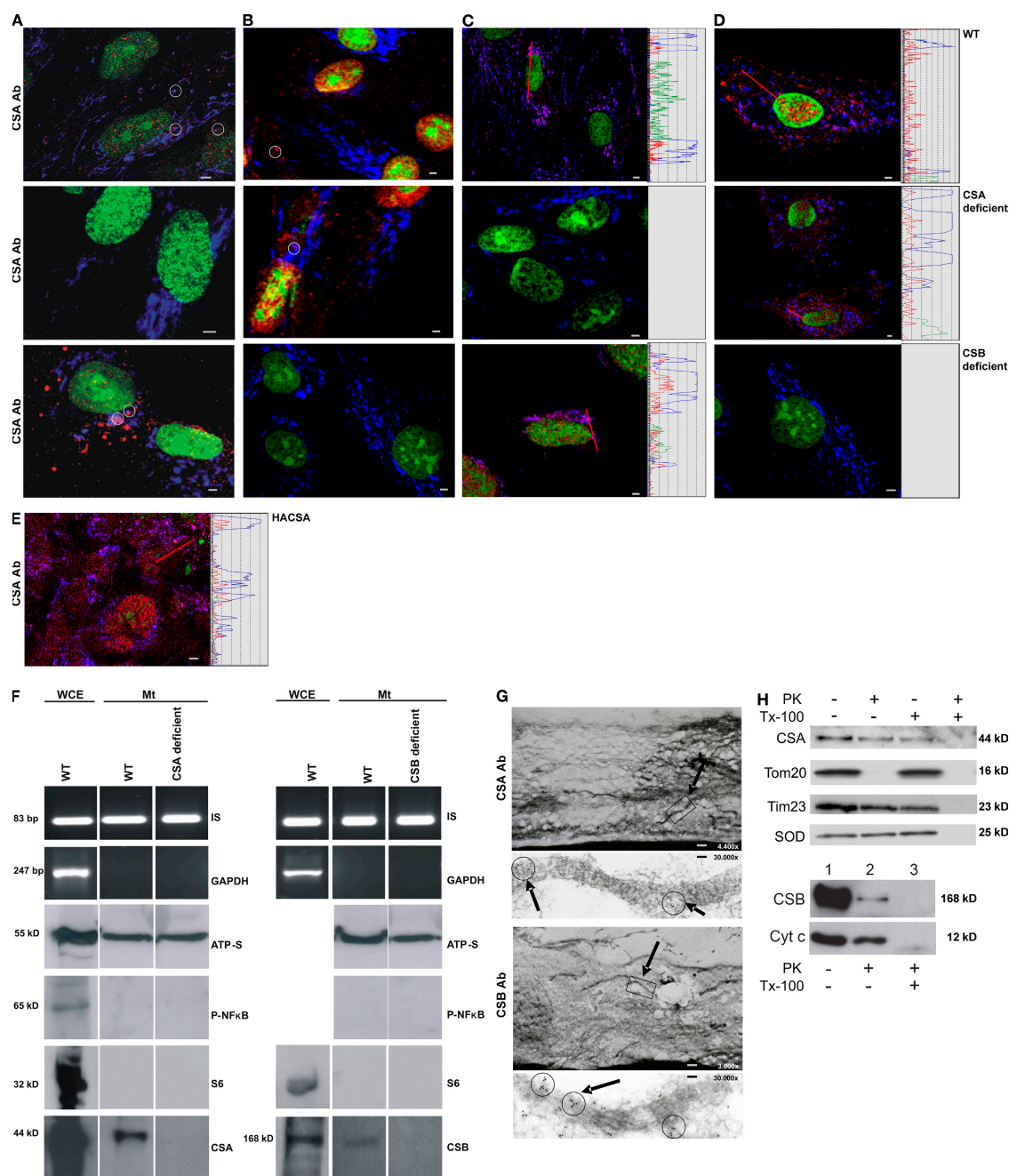
Figure 1. Mitochondrial localization of CSA and CSB in oxidatively stressed cells. Confocal laser scanning microscopy with green fluorescence for nuclear staining, blue fluorescence for mitochondrial staining, and red fluorescence staining for either CSA (A) or CSB (B). Pink fluorescence results from colocalization (white circles) of red mitochondrial CSA/CSB and blue mitochondrial staining. Pictures are representatives of at least five separate experiments. Bar, 1 µm. Exposure of cells to 25 µM H_2O_2 for 12 h leads to signal increase for mitochondrial CSA (C) and CSB (D). Histograms show signal intensities along the red line in the picture with simultaneous signal increment. (E) CSA-deficient fibroblasts transfected with CSA WT protein. Pictures are representatives of at least three independent experiments. Bar, 1 µm. (F) Whole-cell extracts (WCE) and mitochondrial extracts (Mt) prepared from H_2O_2-treated cells. Presence of mtDNA (IS) and absence of nuclear DNA (GAPDH), shown by PCR. Immunoblotting of mitochondrial ATP-synthetase β, phospho-NF-κB, S6, CSA, and CSB. Pictures are representatives of at least three independent experiments. (G) Electron microscopic image of oxidatively stressed normal human fibroblasts stained with gold-labeled (circles) CSA (top) or CSB (bottom). Bars: (top CSA image) 1.1 µm; (top CSB image) 1.6 µm; (bottom) 165 nm. Electron micrographs are representatives of at least two separate experiments. (H) Top: mt (10 µg protein per lane) isolated from H_2O_2-treated WT cells were incubated where indicated with 100 µg/ml proteinase K (PK) in the presence or absence of Triton X-100 (Tx-100). SDS-PAGE of mitochondrial proteins with antibodies against CSA, Tom20, Tim23, and superoxide dismutase (SOD). Bottom: mt (25 µg per lane) isolated from H_2O_2-treated WT cells were incubated with 25 µg/ml proteinase K (PK) in the presence or absence of Triton X-100 (Tx-100). SDS-PAGE of mitochondrial proteins with antibodies against CSB and cytochrome C. Pictures are representatives of at least two independent experiments.

The NER proteins CSA and CSB interact with the BER protein mtOGG1 and mtSSBP1 in a complex with mtDNA

The presence of mtOGG-1 and mt single stranded DNA binding protein (mtSSBP)-1 in mt and their role in repair of oxidative mtDNA damage have previously been shown (Nishioka et al., 1999; de Souza-Pinto et al., 2001). Therefore, we investigated, if CSA and CSB directly interact with mtDNA, mtOGG-1 and mtSSBP-1 (Fig. 2). To assess binding to mtDNA and the proteins indicated, gel electrophoresis mobility shift assays (GEMSAs; Fig. 2 A), as well as coimmunoprecipitation (CoIP; Fig. 2, B–E) experiments were performed. In GEMSA experiments, labeled mtDNA shifted in the presence of extracts generated from oxidatively stressed mt with a supershift in the presence of CSA antibody (arrow; Fig. 2 A). This supershift is consistent
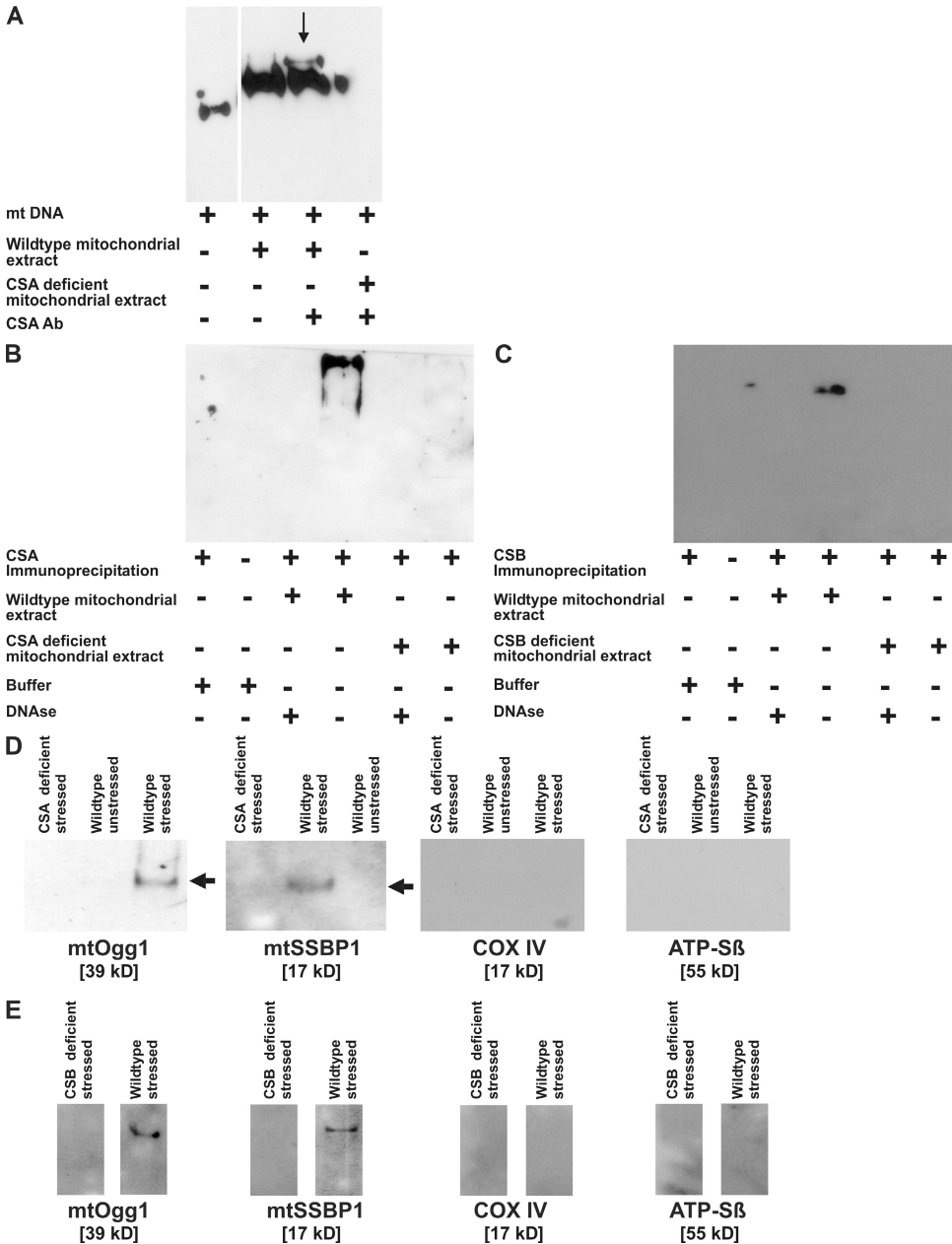

Figure 2. Complex formation of CSA/CSB proteins with mtDNA as well as mtOgg1 and mtSSBP1 in oxidatively stressed mt. (A) GEMSA: Biotin-labeled mtDNA was incubated with mitochondrial extracts of oxidatively stressed normal or CSA-deficient human cells and with subsequent PAGE. Incubation with CSA antibody in WT mitochondrial extract showed a supershift (arrow). CoIP with biotin-labeled mtDNA. CoIP of CSA– (B) or CSB–mtDNA (C) complexes occurred only in WT mitochondrial extracts but vanished under DNase digestion. Complexes containing mtOgg1, mtSSBP1, COXIV, and ATP-Sβ were extracted by CoIP from mitochondrial extracts of CSA- and CSB-deficient and WT cells, exposed to 30 µM H_2O_2. The presence of CSA (D) and CSB (E) could be detected in complex with mtOgg1 and mtSSBP1 (arrows) by Western blot. Pictures are representatives of at least three independent experiments.

with the presence of CSA in a mtDNA–protein complex. To confirm these results, CSA-containing protein complexes were immunoprecipitated and the presence of mtDNA was shown by DNA-specific biotin labeling. MtDNA could only be detected in CSA-containing protein complexes of oxidatively stressed mt from normal human cells in the absence of DNase digestion (Fig. 2 B). There was no detectable CoIP of CSA–mtDNA complexes in CSA-deficient extracts, in unstressed mitochondrial extracts, or in negative buffer controls, and treatment of the CSA precipitates with DNase digestion abolished the signal. CSB–mtDNA complexes were equally detectable by CoIP (Fig. 2 C). To assess direct interaction with other known mitochondrial proteins, CoIP was performed for mtOGG-1, mtSSBP-1, cytochrome oxidase (COX) IV, and ATP-Synthase (ATP-S) subunit β with CSA (Fig. 2 D) and CSB (Fig. 2 E). DNase digestion–resistant interaction of NER–associated CSA and CSB in oxidatively stressed mt could clearly be detected for mtOGG-1 and mtSSBP-1, but not for COX IV or ATP-Sβ. Such an interaction could not be shown in CSA- or CSB-deficient cells (Fig. 2, D and E, respectively). Interaction did not occur in nonstressed mt. Thus, simple binding of proteins on mtDNA at distant sites can be excluded (unpublished data).

Accelerated induction of aging–associated mtDNA mutations in CSA and CSB cells

The 4,977 bp "common" deletion of mtDNA can be generated through oxidative stress and is considered to be a marker for the presence of other mtDNA mutations (Balajee et al., 1999; Berneburg et al., 1997, 2004). The potential role of CSA and CSB proteins in protection from damage of mtDNA was assessed by repetitive exposure of normal human fibroblasts, as well as CSA- and CSB-deficient fibroblasts to sublethal UVA-irradiation and subsequent screening for mtDNA mutations using quantitative real-time PCR, as previously published (Berneburg et al., 1997, 1999, 2004, 2005; Koch et al., 2001).

We and others have shown that repetitive, nonlethal UVA irradiation induces the common deletion in normal human fibroblasts and keratinocytes after 2 wk of irradiation (Berneburg et al., 1999, 2005; Koch et al., 2001). When compared with normal human and XP-D fibroblasts, exposure of either CSA- or CSB-deficient fibroblasts to this treatment regimen prematurely induced the common deletion. More importantly, the relative frequency of mtDNA deletions was up to 10-fold higher than in normal human fibroblasts (Fig. 3). Addition of exogenous ROS scavengers can protect against UVA-induced mtDNA deletions (Berneburg et al., 1999). If the CS proteins are involved in protection from oxidative mtDNA damage, ROS scavengers should also compensate for the deficiency of CS fibroblasts. In fact, coincubation of repetitively irradiated CSA-deficient cells with vitamin E protected from induction of mtDNA mutagenesis, indicating that CSA is involved in protection from mtDNA damage resulting from oxidative stress (Fig. 3). To provide formal proof of this hypothesis, we transfected

CSB-deficient fibroblasts with the WT *CSB* gene and exposed the cells to oxidative damage using repetitive UVA irradiation. Indeed, complementation of CSB deficiency reduced the frequency of mtDNA mutations to the level of normal human cells.

Age dependent accumulation of mtDNA mutations in the subcutaneous fat tissue of *Csb^m/m^* and *Csa^−/−^* mice

Photosensitivity of CS patients is currently explained by the known deficiency of CS cells in TC-NER. However, other age-associated symptoms such as reduced subcutaneous fat tissue cannot readily be deduced from this. To investigate whether mtDNA mutations are associated with this particular progeroid symptom in vivo, microdissected subcutaneous fat tissue from mice lacking the functional *Csb* or *Xpa* gene were assessed for the present levels of the most frequent mouse-mtDNA deletion in comparison to WT littermate controls, depending on their respective ages. Tissues from mice aged 13, 52, and 130 wk were
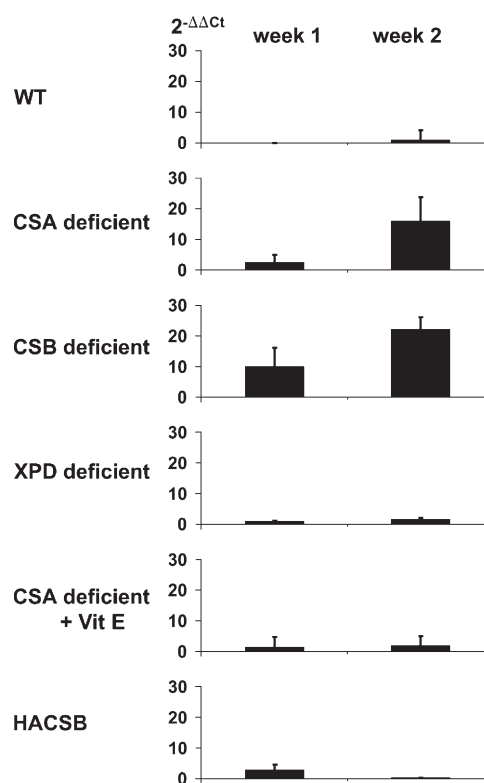

Figure 3.   Accelerated induction of mt mutations in UVA–irradiated CSA– and CSB–deficient cells. Primary human fibroblasts of two and three patients suffering from CSA and CSB, respectively, one XP patient (XP-D), and three normal individuals were irradiated with UVA and the relative amount of common deletion was assessed by quantitative real-time PCR. Levels of the common deletion are given in $2^{-\Delta\Delta Ct}$ as mean ± SD of at least three separate experiments. Levels above one indicate a higher amount of common deletion in UVA-treated cells relative to untreated control cells. Premature UVA-mediated induction of common deletion in CSA cells can be attenuated by treatment with the radical scavenger vitamin E. Expression of HA-tagged CSB protein in CSB-deficient cells lead to normalization of mitochondrial mutagenesis.

investigated. Overall, there was an age-dependent accumulation of mtDNA mutations in all mice investigated. In addition to this, the $Csb^{m/m}$ mice show a strong increase of the mtDNA deletion in subcutaneous fat tissue of aged mice that exceeded levels of 60% in all $Csb^{m/m}$ animals (Fig. 4 A). This effect was highly

significant (P < 0.01, Student's t test) when comparing $Csb^{m/m}$ with WT and $Xpa^{-/-}$ mice at 130 wk of age. Morphologically, this correlated with reduced subcutaneous fat tissue in histological sections of $Csb^{m/m}$ mice at the age of 130 wk (Fig. 4 B), whereas WT and $Xpa^{-/-}$ animals did not show this phenotype.
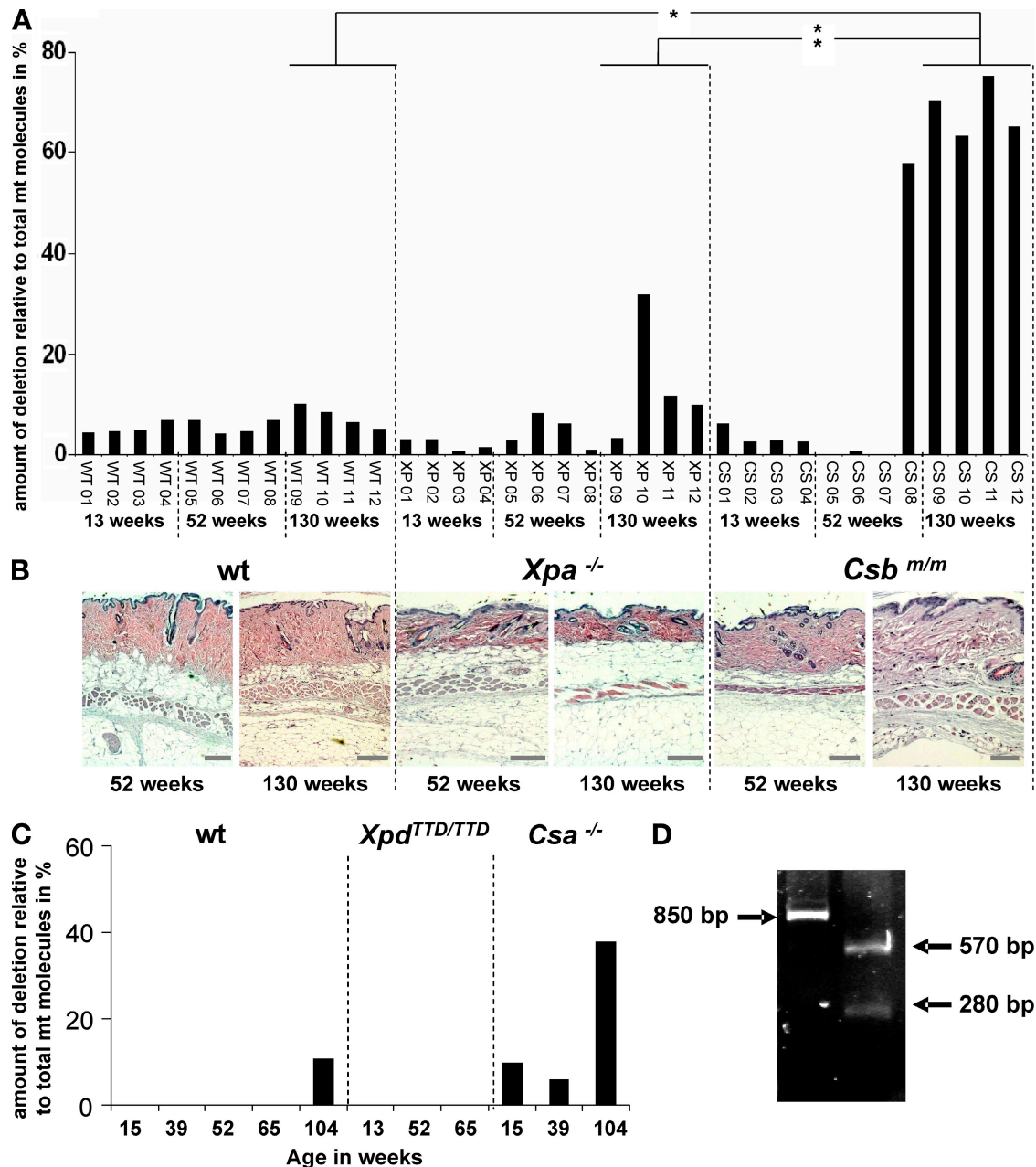

Figure 4. Age dependent accumulation of mtDNA mutations in subcutaneous fat tissue of $Csb^{m/m}$ and $Csa^{-/-}$ mice. (A) Subcutaneous fat tissue from WT mice and mice lacking a functional Csb or the Xpa gene were assessed for a frequent mouse-mtDNA deletion (D17). Three age groups (13, 5, and 130 wk, 4 mice per group) of each genotype were investigated. Aged $Csb^{m/m}$ mice show a strong increase of D17 in subcutaneous fat compared with WT or $Xpa^{-/-}$ controls (Student's t test, P < 0.01). Each PCR experiment was repeated independently two times. (B) Hematoxylin and eosin–stained cross sections with reduced subcutaneous fat tissue in old $Csb^{m/m}$ mice aged for 130 wk. Bar, 200 μm. (C) Measurement of D17 deletion in subcutaneous fat of WT, $Csa^{-/-}$ and $Xpd^{TTD/TTD}$ mice similar to A. Each PCR experiment was repeated independently two times. (D) Restriction digest of PCR product of deletion D17 with EcoRV. (left) Undigested fragment of 850 bp. (right) EcoRV digest leading to fragments of 570 and 280 bp. Data are given as representative of at least three independent experiments.

Increased mitochondrial mutations in subcutaneous fat tissue could also be detected in $Csa^{-/-}$ mice (Fig. 4 C). There was a strong increase of mtDNA mutations in 104-wk-old $Csa^{-/-}$ mice, whereas no increased levels were detected in younger animals, WT, as well as $Xpd^{TTD/TTD}$ mice.

All PCR results could be confirmed by sequence analysis (not depicted), as well as by restriction enzyme digested with EcoRV (Fig. 4 D) and PacI (not depicted). Similar results were obtained with another mt deletion D1 (Fig. S3) as described by Tanhauser and Laipis (1995).

Aging–associated loss of subcutaneous fat tissue is mediated on the cellular level by increased cellular turnover. Oxidatively stressed fibroblasts containing high levels of mtDNA deletions show increased apoptosis

To address the question whether reduction of subcutaneous fat occurs via reduction of fat cell size or via reduction of fat cell number, we performed Ziehl-Neelsen staining for lipofuscin of subcutaneous fat tissue from 130-wk-old $Csb^{m/m}$ mice containing high levels of mtDNA deletions (Fig. 5 A). There was an increased level of macrophages

Figure 5.   Aging–associated loss of subcutaneous fat tissue is mediated on the cellular level by increased cellular turnover. Oxidatively stressed fibroblasts containing high levels of mtDNA deletions show increased apoptosis. (A) Ziehl-Neelsen staining for lipofuscin of subcutaneous fat tissue from 130-wk-old $Csb^{m/m}$ mice containing high levels of mtDNA deletions (6 WT and 4 $Csb^{m/m}$ mice were investigated). Increased level of macrophages containing granular lipofuscin (arrowheads) and no increase in normal fat cells (asterisks). Arrow points to hair follicle. Bar, 50 μm. (B) Quantification of histological sections of lipofuscin-positive macrophages from A with 17% (1 of 6 individuals) of histological sections with lipofuscin-positive cells (macrophages) in WT and 75% (3 of 4 individuals) in $Csb^{m/m}$ mice. (C) FACS analysis for annexin V–positive and propidium iodide (PI) negative (apoptotic) cells with (black bars) or without (gray bars) 2 wk of UVA irradiation. Increase of apoptotic cells in CSA- and CSB-deficient cells compared with WT and nonirradiated controls. Data are representative of at least three separate experiments.

containing granular lipofuscin, whereas levels in normal fat cells were not increased (Fig. 5 B), indicating phagocytosis of cell debris. To investigate whether this may be caused by apoptosis of fat cells containing excessive levels of mtDNA mutations, we FACS-sorted UVA-irradiated fibroblasts (Fig. 5 C) and observed that CSA- and CSB-deficient fibroblasts containing high levels of mtDNA mutations undergo apoptosis at higher levels compared with WT cells containing lower levels of mtDNA mutations. This increased apoptotic cell death especially occurred in cells containing high levels of mtDNA deletions. Nonirradiated controls showed WT levels of apoptosis.

DISCUSSION

Analysis of unstressed normal human cells did not reveal a clear detectable signal for CSA and CSB proteins in mt. However, exposure of cells to oxidative stress induced by UVA or H_2O_2 showed a marked enrichment of both proteins in mt as shown by three different approaches, and in at least two different cell lines for each complementation group.

Whereas early work demonstrated no removal of cyclobutyl pyrimidine dimers and 6–4 photoproducts by NER in mt (Clayton et al., 1974; Pascucci et al., 1997), removal of oxidative damage in mt has been linked to presence of BER components (Bogenhagen et al., 2001; de Souza-Pinto et al., 2001). Interestingly, a role for CSA and CSB in repair of oxidative damage of nuclear DNA has been reported (Le Page et al., 2005; D'Errico et al., 2007; Stevnsner et al., 2008), and the presence of CSA and CSB in mt has been postulated previously, yet direct evidence has remained elusive, possibly because of low baseline levels. Low amounts at baseline and absence of mitochondrial targeting sequences (MTS) may account for lacking detection of CS proteins in mt under unstressed conditions by standard methods, including yeast proteomics (Reinders et al., 2006), although alternative import mechanisms remain possible (Stojanovski et al., 2007). Although the exact mechanism of mitochondrial import of CSA and CSB is not clear, one can speculate that upon stress conditions, a conformational change in these proteins and/or specific modification results in the formation of an internal mitochondrial targeting signal. Analysis of the primary sequence of both CSA and CSB with a program aimed at prediction of mitochondrial targeting signals (MitoProt II) suggested that such a canonical signal is not present in these proteins. The absence of an N-terminal cleavable targeting sequence is supported by our observation that the mitochondrial portion of the protein does not migrate faster on SDS-PAGE than the bulk of the protein which is obtained in the whole cell extract (Fig. 1 F). Furthermore, sequence analysis did not reveal splice variants which result in mitochondrial targeting signals. The majority of the CSB molecules were sensitive to protease treatment (Fig. 1 H). This observation suggests that only a small portion of the molecules are in internal compartments of the organelle, whereas the vast majority of the mitochondrial–associated protein is on the surface or in the process of being imported into the organelle. Thus,
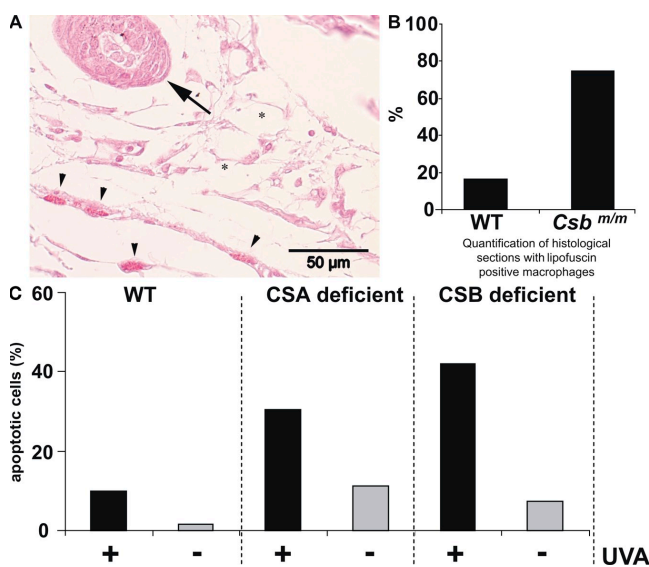
this outer-surface portion could represent a CSB pool of protein, ready to be imported into mt. Of note, CSA and CSB synthesized in a cell-free system could not be imported in vitro into mt isolated from fibroblasts (unpublished data). Thus, as observed in many cases in the past, it appears that the in vitro system cannot resemble the situation in intact cells.

Mitochondrial enrichment of CSA and CSB after exposure to different sources of oxidative stress indicates a functional role of CS proteins in damage processing. This enrichment cannot be explained by simple increased permeability of mt caused by treatment with H_2O_2 or UVA, as viability of cells was not affected by the oxidative stress applied and the mitochondrial marker ATP-synthetase was not detected in the cytoplasm by confocal microscopy. In addition to this, localization assays and immunoelectronmicroscopy experiments directly demonstrated localization of CSA and CSB proteins inside the mt rather than simple attachment to the outer mitochondrial membrane. This strongly supports our proposal that the CSA and CSB proteins are physically present inside mt, a localization in close proximity to mtDNA.

Mt do contain mtOGG-1, and this enzyme has been shown to be involved in repair of oxidative mtDNA damage (de Souza-Pinto et al., 2001). Furthermore, interaction of CSB with nuclear components of BER has been reported (Muftuoglu et al., 2009). In contrast, a direct interaction of mitochondrial NER–associated CSA and CSB and BER–associated mtOGG-1 and mtSSBP-1 in mt has not been shown previously. In the present study, GEMSA showed direct interaction of CSA with mtDNA of oxidatively stressed mt and CoIP experiments revealed a direct interaction of CSA and CSB with mtDNA, mtOGG-1, and mtSSBP-1. Recent work indicates separable roles for CSA in the cellular response to UV and oxidative DNA damage (Nardo et al., 2009) and mitochondrial dysfunction mediated by CSB deficiency in the pathology of CS (Osenbroch et al., 2009). Our experiments support this notion because neither CSA nor CSB interact with COX IV and ATP-Sβ upon oxidative stress. Furthermore, we could previously show that sublethal levels of oxidative stress do not significantly reduce cellular ATP-levels in human cells (Berneburg et al., 2005). Therefore, our data also argue for specific roles of CSA and CSB in response to oxidative stress by direct interaction of NER-CSA and NER-CSB with BER-mtOGG-1.

Mutations of mitochondrial DNA are involved in neurodegenerative processes (Kraytsberg et al., 2006; Lin and Beal, 2006), as well as normal aging (Schriner et al., 2005; Trifunovic et al., 2004) and premature aging of the skin (Pang et al., 1994; Berneburg et al., 1997, 1999, 2004, 2005; Koch et al., 2001; Durham et al., 2003). Accelerated induction of the "common" mtDNA deletion in deficient CSA and CSB cell lines provides evidence for a role of CS proteins in counteracting mitochondrial mutagenesis. The exact role of CSA and CSB in the mitochondrion is not clear, but delay of mtDNA mutagenesis by vitamin E indicates a role in protection from oxidatively induced mtDNA damage. Although it has been shown that in $Ogg1^{-/-}/Csb^{-/-}$ double-knockout

mice the basal levels of 7,8-dihydro-8-oxoguanine (8-oxoG) and other oxidative modifications in mtDNA are low (Trapp et al., 2007), others demonstrated deficient mitochondrial repair of 8-oxoG in $Csb^{-/-}$ mouse cells and CSB-deficient human fibroblasts (Stevnsner et al., 2002). This may be caused by higher levels of 8-oxoG lesions on transfected plasmids. In our system, under oxidative stress we found premature induction of mtDNA deletions reported to be triggered by oxidative stress to be directly dependent on CS proteins because it was not detectable in NER-deficient XP-D mutated cells, but it was in CSB-deficient cells, and it was normalized by stable expression of HA-tagged CSB in CSB-deficient fibroblasts.

The fact that XP-D–mutated cells show WT levels of mtDNA deletions upon irradiation (Fig. 3) indicates that at least this protein is not necessary for protection from oxidatively induced mtDNA mutations. Together with the fact that CPD are not removed from mtDNA (Clayton et al., 1974), this indicates that there is no NER as such in mt. Whether other NER–associated proteins are present in mt remains to be determined.

Patients suffering from CS show growth and mental retardation and sensitivity of the skin to UV radiation. Interestingly, one of the most prominent clinical progeroid symptoms in CS is loss of subcutaneous fat tissue (Berneburg and Lehmann, 2001; van Hoffen et al., 2003; van der Wees et al., 2007). Particularly, age-associated loss of subcutaneous fat, especially of the buccal region is a prominent feature of normal aging. This is where loss of subcutaneous fat tissue in CS-deficient mice was also most prominent. Extrinsically aged (photoaged) skin shows increased frequencies of functionally relevant mtDNA mutations (Berneburg et al., 1997, 2004; Durham et al., 2003). In line with the notion that mtDNA mutations and age-dependent loss of subcutaneous tissue are causally linked, highly elevated levels of mtDNA mutations were found in reduced subcutaneous fat tissue of aged $Csa^{-/-}$ and $Csb^{m/m}$ mice, particularly in the buccal region, where loss of subcutaneous tissue was most prominent. The magnitude of mtDNA mutational levels with more than 40% ($Csa^{-/-}$) to 60% ($Csb^{m/m}$) of the mitochondrial genome being mutated far exceeded levels previously measured in other tissues under physiological conditions (Berneburg et al., 1997, 1999, 2004, 2005; Durham et al., 2003). This magnitude has only been reported in other genetic diseases caused by mtDNA defects, thus indicating that detected levels of mitochondrial mutations do have direct impact on mitochondrial physiology. Levels of mtDNA mutations in epidermis, dermis, and other organ tissues of aged $Csa^{-/-}$ and $Csb^{m/m}$ mice were much lower than those in subcutaneous tissue, indicating that this is a specific effect for aged subcutaneous fat tissue.

Loss of subcutaneous fat tissue could be mediated via simple reduction of fat content in cells. However, selection on the cellular level against cells containing excessive mtDNA mutations have been reported (Lu et al., 2009). Increased lipofuscin staining pointing to increased cellular turnover in vivo in

386

Cockayne Syndrome A and B in mitochondria | Kamenisch et al.

mice, as well as increased apoptosis in vitro in cells with increased mtDNA mutations indicate aging-associated reduction of subcutaneous fat tissue via a mechanism that involves apoptotic cell loss. Although we cannot entirely rule out that this apoptotic cell loss is mediated by nuclear signals, the fact that apoptosis was especially detectable in irradiated fibroblasts with high levels of mtDNA deletions, and because high levels of mtDNA deletions have been shown to induce apoptotic cell death independent from nuclear signals (Bravo-Nuevo et al., 2003; Zanna et al., 2003; Dubec et al., 2008), in our eyes, it is more likely that this was mediated via mitochondrial signals.

In conclusion, these data suggest that the CSA and CSB proteins are not only present in the nucleus but they are also recruited to the mitochondrion upon oxidative stress. Mechanistically, CSA and CSB (a) directly interact with mtDNA and BER-associated mtOGG-1, as well as mtSSBP-1, (b) are involved in protection from oxidatively induced and aging-associated mtDNA mutations, and (c) protect against the age-associated reduction of subcutaneous fat tissue in $Csa^{-/-}$ and $Csb^{m/m}$ mice (d) via a mechanism involving increased cell turnover.

This study links a novel role of intramitochondrial CS proteins, namely the protection from oxidative mtDNA damage, to reduced subcutaneous fat tissue as segmental progeroid symptom in CS patients with implications for normal human aging, and this is performed via a mechanism using the NER proteins CSA and CSB, as well as the BER protein mtOGG-1 together with mtSSBP-1. Whether this is performed by a strong link between NER and BER remains to be shown, and the exact mechanistic function of CSA and CSB as well as the specific form of interaction with other proteins in mt still needs to be established.

MATERIALS AND METHODS

Human and animal material. Human and animal protocols were approved by the local ethics committee of the Eberhard Karls University, Tübingen, Germany.

Cell culture. Primary fibroblasts from normal individuals (F92, FF3, C5ROWT) and CSB patients (CS1TAN, GM739), CSA patients (CS6BR, CS3BE), and XP-D–mutated cells were cultured in Eagle's minimum essential medium (Life Technologies GmbH) containing 15% fetal calf serum (Greiner), 1% L-Glutamine, and 1% Streptomycin/Amphotericin B (Invitrogen) in a humidified atmosphere containing 5% CO_2. In addition, CSB cells (CS1AN SV-40 transformed) complemented with HA-tagged CSB (HACSB) and CSA cells (CS3BE SV-40 transformed) complemented with HA-tagged CSA (HACSA) were used. Cells were kept in 10- or 15-cm culture dishes for culture and irradiation. All cell lines used are listed in Table S1.

Chemical treatments. All chemicals were purchased from Sigma-Aldrich and applied as described previously (Berneburg et al., 1997, 1999, 2004, 2005) or as indicated.

Isolation of mt. Mt were isolated as described earlier (Jensen et al., 2003; Schriner et al., 2005). All steps are performed on ice. In brief, 5×10^6 cells were trypsinized and pelleted with subsequent washing in Mito-Isolation buffer (210 mM mannitol, 70 mM sucrose, 1 mM EGTA, and 5 mM Hepes). Cell pellets were broken up by Digitonin (Sigma-Aldrich) and repeated mechanical treatment using a Teflon-homogenizer (Potters). Separation of mt from cell debris was achieved by multiple wash steps with Mito-Isolation buffer, taking mt from the supernatant. Final centrifugation at 10,000 rpm for 20 min in Mito-Isolation buffer yields mitochondrial pellet.

Protein extracts. All procedures were performed on ice or at 4°C using ice-cold buffers.

For the preparation of whole-cell extracts, 5×10^6 cells were trypsinized, and washed twice with wash buffer (210 mM mannitol, 70 mM sucrose, 1mM EGTA, 10 mM Hepes-KOH, pH 7.9, and 0.5% BSA). After the first wash, 1/30 of the (cell suspension) volume was pelleted and resuspended in lysis buffer (10 mM Hepes-KOH, pH 7.9, 0.45 M NaCl, 10% glycerol, 210 mM mannitol, 70 mM mucrose, 1 mM EGTA, 1 mM PMSF, and 1 mM DTT), while the rest was used for the isolation of mt extracts. The cell suspension was freeze-thawed 3 times (snap-freeze in liquid nitrogen/thaw at 30°C for 5 min) and the supernatant, obtained after centrifugation (10,000 rpm, 10 min), was used as whole-cell extract.

For the preparation of mitochondrial extracts, the mitochondrial pellet, isolated as described above, was resuspended in 50 µl Mito-Isolation buffer and incubated on ice for 15 min. The mitochondrial extracts with protein concentrations of 8 µg/µl were enriched with 5% BSA solution.

Antibodies and immunoblot analysis. We used two types of antibodies for the immunodetection of the CSB protein (Santa Cruz Biotechnology, Inc.) and two types of antibodies for the immunodetection of the CSA protein (Santa Cruz Biotechnology, Inc. and Biozol). All antibodies used are given in Table S3. The analysis of the different protein extracts for the presence of CSA, CSB and XPA proteins was performed by immunoblotting with chemiluminescent detection (ECL-plus; GE Healthcare). Equal amount of proteins were separated on 8% SDS-PAGE gels for the CSB protein and 12% for the CSA and transferred to Immobilon-P membranes using 1 X Transfer buffer (25 mM Tris, 0.2 M Glycine, 20% Methanol, and 0.1% SDS, pH 8.5). The membranes were incubated overnight with the primary antibodies and for 45 min with the corresponding horseradish peroxidase-conjugated secondary antibodies.

Protease treatment of isolated mt. Isolated mt were treated with 25 mg/ml proteinase K in SEM buffer (250mM sucrose, 1 mM EDTA, and 10 mM MOPS, pH 7.2) in the absence or presence of 1% Triton X-100 for 15 min at 4°C. Proteinase K was inactivated by the addition of PMSF to a final concentration of 4 mM. The samples were incubated for 10 min at 4°C. Mt were reisolated and washed with SEM buffer. In the case of Triton lyses, the supernatant was used directly for SDS-PAGE analyzes. Proteins were loaded on a 15% SDS-PAGE and analyzed by Western blotting and immunodecoration.

GEMSA. Procedures were conducted as described in the manufacturer's protocol (Thermo Fisher Scientific). In brief, mitochondrial extracts of oxidatively stressed fibroblasts were incubated with biotin labeled and purified mtDNA fragment (Biotin 3′ End Labeling kit; Thermo Fisher Scientific) for 20 min at 37°C, followed by incubation in the presence or absence of CSA antibody for 10 min at 37°C. Subsequently, the samples were separated by gel electrophoresis using an 8% native acrylamide gel at 120 V for 1 h in TBE buffer. MtDNA–protein complexes were blotted to a nylon membrane (Roth) at 200 mA for 1 h in TBE buffer. Shifted or supershifted biotin-labeled mtDNA was detected using a chemiluminescent nucleic acid detection module (Thermo Fisher Scientific).

CoIP. CSA protein-containing complexes were isolated from mitochondrial extracts of oxidatively stressed fibroblasts with CSA antibody-associated protein A/G beads (Thermo Fisher Scientific) in PBS. Isolated CSA complexes were washed five times with cold PBS, and coprecipitated mtDNA

was labeled with biotin (Biotin 3′ End Labeling kit) and incubated with or without DNase (rDNase; Machery-Nagel) for 15 min at room temperature. Samples were separated by gel electrophoresis in an 8% native acrylamide gel at 120 V for 1 h in TBE buffer. DNA–protein complexes were blotted to a nylon membrane at 200 mA for 1 h in TBE buffer. Biotin-labeled mtDNA associated to the CSA complex was detected using a chemiluminescent nucleic acid detection module.

UVA irradiation. Repetitive UVA irradiation was performed as described previously (Berneburg et al. 1999, 2005). In brief, for UVA irradiation, medium was replaced by PBS, lids were removed, and cells were exposed to radiation from a Sellamed 24000 (Sellas Medical Devices). The emission was filtered with UVACRYL (Mutzhas) and UG1 (Schott Glaswerke) and consisted of wavelengths >340 nm. The UVA output was determined with a UVAMETER (Mutzhas) and found to be ∼70 mW/cm² UVA at a tube-to-target distance of 30 cm.

To induce mtDNA mutations, cells were irradiated 3 times daily with 8 J/cm² UVA for 4 consecutive days and checked for viability by trypan blue exclusion. Cells were then aliquoted equally with one aliquot stored at −80°C until extraction of mtDNA and another aliquot plated to a 10-cm culture dish for ongoing culture and irradiation.

DNA extraction. Total cellular DNA was extracted as described previously (Berneburg et al., 1997, 1999, 2004, 2005).

Quantitative real-time PCR. Detection of the mt common deletion was performed by real-time PCR as described previously (Koch et al., 2001). The normalized level of common deletion in UVA-irradiated cells (ΔCt) was compared with the corresponding normalized common deletion level of (sham-irradiated) unirradiated cells (controls), resulting in $\Delta\Delta Ct$ value. Levels of common deletion in UVA-irradiated cells in relation to unirradiated cells are given as base of 2 and the negative power of $\Delta\Delta Ct$ values ($2^{-\Delta\Delta Ct}$), as described previously (Koch et al., 2001; Berneburg et al., 2004).

Mouse PCR. Whole-skin samples from WT, $xpa^{-/-}$, and $csb^{-/-}$ mice of different age groups (13, 52, and 130 wk) were microdissected under microscopic control to isolate subcutaneous tissue free of other tissue contamination. From these samples, mtDNA was extracted and detection of the mouse mtDNA deletion (D17 and D1) was performed as described previously (Tanhauser and Laipis, 1995). In brief, after DNA extraction and subsequent PCR, levels of mouse mtDNA deletion (D17 and D1) and undeleted mitochondrial DNA sequences were measured densitometrically by phosphorimager analysis. The correct sequence of PCR products was verified by DNA sequencing and digestion with restriction enzymes EcoRV and PacI (New England Biolabs). Values of mouse mtDNA deletion (D17 and D1) were normalized against corresponding values of undeleted mitochondrial DNA sequences.

Immunofluorescence analysis. Cells grown on chamber slides (BD) were treated with or without UVA light and fixed in 4% formalin at 4°C for 5 min and methanol at 0°C for 3 min. After permeabilization with 0.25% Triton X-100 in PBS with 1% donkey serum for 10 min, cells were incubated in blocking solution (0.25% Triton X-100 in PBS with 5% donkey serum). Slides were incubated with primary antibodies: mouse anti ATP-Synthetase-β (mitochondrial staining; BD) and rabbit anti-CSA (Biozol and Santa Cruz Biotechnology, Inc.) or goat anti-CSB (Santa Cruz Biotechnology, Inc.) for 2 h at RT. After washing in 0.25% Triton X-100 in PBS with 1% donkey serum for three times, slides were incubated with secondary antibodies: Cy5-labeled donkey anti–mouse and Cy3-labeled donkey anti–goat (Dianova) or Cy3-labeled donkey anti–rabbit (Dianova). Slides were rinsed (0.25% Triton X-100 in PBS with 1% donkey serum) three times and incubated with YOPRO-1 (Invitrogen) for nuclear staining. Cells were rinsed in PBS and mounted in Vectastain mounting media (Vectastain). Cellular fluorescence and localization of CSA or CSB proteins were analyzed using a Leica confocal laser scanning microscope TCS SP (Leica). Three different fluorochromes for nuclear

(YOPRO-1) fluorescence (green), the blue mitochondrial fluorescence (Cy5), and the red fluorescence (Cy3) CSA or CSB proteins were used.

Immunoelectron microscopy (IEM). IEM was performed as described previously (Riess et al., 2004). Cells were fixed in periodate-lysine-paraformaldehyde for 4 h at 4°C and centrifuged. The resulting pellet was embedded in 3.5% agarose at 37°C, and then cooled on ice. Small parts of agarose blocks were dehydrated in ethanol and embedded in Lowicryl K4M (Polysciences). The blocks were cut with an ultramicrotome (Ultracut; Reichert). Ultrathin sections (50 nm) were mounted on formvar-coated nickel grids followed by incubation in blocking solution (PBS with 10% goat or donkey serum). Sections were incubated in goat anti-CSA or rabbit anti-CSB antibodies (Table S3) diluted at a ratio of 1:40 in PBS containing 0.5% BSA for 90 min. The sections were then washed in PBS/BSA. CSA-treated sections were incubated with 6-nm gold-conjugated donkey anti–goat IgG (Dianova) and anti-CSB–treated sections in 10-nm gold-conjugated goat anti–rabbit IgG (GE Healthcare). Antibodies were diluted at a ratio of 1:25 in (PBS/BSA/0.5% Tween 20). In control samples, the primary antibody was omitted. Fixation of the grids in glutaraldehyde was followed by counterstaining with uranyl acetate for 2 min and lead citrate for 30 s. Cellular morphology and localization of CSA or CSB proteins were analyzed using a Zeiss EM 109 transmission electron microscope (Carl Zeiss, Inc.) operating at 80 kV.

Statistical analysis. Average data are presented as mean and SD. Statistical analysis was performed using Excel (Microsoft). For statistical comparison of two groups, we used unpaired, two-tailed Student's t test. Differences were considered highly significant when $P < 0.01$. In the figures, highly significant P values are indicated by two asterisks.

Online supplemental material. Fig. S1 presents the levels of CSA and CSB in mt of unstressed cells without green nuclear staining. Fig. S2 presents the levels of CSA and CSB in oxidatively stressed cells without nuclear green staining. Fig. S3 presents the age dependent accumulation of D1 mtDNA mutation in subcutaneous fat tissue of $Csa^{-/-}$ and $Csb^{m/m}$ mice. Tables S1–S4 describe cell lines, primer oligonucleotides, and antibodies. Online supplemental material is available at http://www.jem.org/cgi/content/full/jem.20091834/DC1.

REFERENCES

Balajee, A.S., I. Dianova, and V.A. Bohr. 1999. Oxidative damage-induced PCNA complex formation is efficient in xeroderma pigmentosum group A but reduced in Cockayne syndrome group B cells. *Nucleic Acids Res.* 27:4476–4482. doi:10.1093/nar/27.22.4476

Berneburg, M., and A.R. Lehmann. 2001. Xeroderma pigmentosum and related disorders: defects in DNA repair and transcription. *Adv. Genet.* 43:71–102. doi:10.1016/S0065-2660(01)43004-5

Berneburg, M., N. Gattermann, H. Stege, M. Grewe, K. Vogelsang, T. Ruzicka, and J. Krutmann. 1997. Chronically ultraviolet-exposed human skin shows a higher mutation frequency of mitochondrial DNA as compared

to unexposed skin and the hematopoietic system. *Photochem. Photobiol.* 66:271–275. doi:10.1111/j.1751-1097.1997.tb08654.x

Berneburg, M., S. Grether-Beck, V. Kürten, T. Ruzicka, K. Briviba, H. Sies, and J. Krutmann. 1999. Singlet oxygen mediates the UVA-induced generation of the photoaging-associated mitochondrial common deletion. *J. Biol. Chem.* 274:15345–15349. doi:10.1074/jbc.274.22.15345

Berneburg, M., H. Plettenberg, K. Medve-König, A. Pfahlberg, H. Gers-Barlag, O. Gefeller, and J. Krutmann. 2004. Induction of the photo-aging-associated mitochondrial common deletion in vivo in normal human skin. *J. Invest. Dermatol.* 122:1277–1283. doi:10.1111/j.0022-202X.2004.22502.x

Berneburg, M., T. Gremmel, V. Kürten, P. Schroeder, I. Hertel, A. von Mikecz, S. Wild, M. Chen, L. Declercq, M. Matsui, et al. 2005. Creatine supplementation normalizes mutagenesis of mitochondrial DNA as well as functional consequences. *J. Invest. Dermatol.* 125: 213–220.

Bogenhagen, D.F., K.G. Pinz, and R.M. Perez-Jannotti. 2001. Enzymology of mitochondrial base excision repair. *Prog. Nucleic Acid Res. Mol. Biol.* 68:257–271. doi:10.1016/S0079-6603(01)68105-4

Bravo-Nuevo, A., N. Williams, S. Geller, and J. Stone. 2003. Mitochondrial deletions in normal and degenerating rat retina. *Adv. Exp. Med. Biol.* 533: 241–248.

Clayton, D.A., J.N. Doda, and E.C. Friedberg. 1974. The absence of a pyrimidine dimer repair mechanism in mammalian mitochondria. *Proc. Natl. Acad. Sci. USA.* 71:2777–2781. doi:10.1073/pnas.71.7.2777

D'Errico, M., E. Parlanti, M. Teson, P. Degan, T. Lemma, A. Calcagnile, I. Iavarone, P. Jaruga, M. Ropolo, A.M. Pedrini, et al. 2007. The role of CSA in the response to oxidative DNA damage in human cells. *Oncogene.* 26:4336–4343. doi:10.1038/sj.onc.1210232

de Souza-Pinto, N.C., L. Eide, B.A. Hogue, T. Thybo, T. Stevnsner, E. Seeberg, A. Klungland, and V.A. Bohr. 2001. Repair of 8-oxodeoxyguanosine lesions in mitochondrial DNA depends on the oxoguanine DNA glycosylase (OGG1) gene and 8-oxoguanine accumulates in the mitochondrial DNA of OGG1-defective mice. *Cancer Res.* 61:5378–5381.

Dubec, S.J., R. Aurora, and H.P. Zassenhaus. 2008. Mitochondrial DNA mutations may contribute to aging via cell death caused by peptides that induce cytochrome c release. *Rejuvenation Res.* 11:611–619. doi:10.1089/rej.2007.0617

Durham, S.E., K.J. Krishnan, J. Betts, and M.A. Birch-Machin. 2003. Mitochondrial DNA damage in non-melanoma skin cancer. *Br. J. Cancer.* 88:90–95. doi:10.1038/sj.bjc.6600773

Furuta, T., T. Ueda, G. Aune, A. Sarasin, K.H. Kraemer, and Y. Pommier. 2002. Transcription-coupled nucleotide excision repair as a determinant of cisplatin sensitivity of human cells. *Cancer Res.* 62:4899–4902.

Jensen, A., G. Calvayrac, B. Karahalil, V.A. Bohr, and T. Stevnsner. 2003. Mammalian 8-oxoguanine DNA glycosylase 1 incises 8-oxoadenine opposite cytosine in nuclei and mitochondria, while a different glycosylase incises 8-oxoadenine opposite guanine in nuclei. *J. Biol. Chem.* 278:19541–19548. doi:10.1074/jbc.M301504200

Kamiuchi, S., M. Saijo, E. Citterio, M. de Jager, J.H. Hoeijmakers, and K. Tanaka. 2002. Translocation of Cockayne syndrome group A protein to the nuclear matrix: possible relevance to transcription-coupled DNA repair. *Proc. Natl. Acad. Sci. USA.* 99:201–206. doi:10.1073/pnas.012473199

Koch, H., K.P. Wittern, and J. Bergemann. 2001. In human keratinocytes the Common Deletion reflects donor variabilities rather than chronologic aging and can be induced by ultraviolet A irradiation. *J. Invest. Dermatol.* 117:892–897. doi:10.1046/j.0022-202x.2001.01513.x

Kraytsberg, Y., E. Kudryavtseva, A.C. McKee, C. Geula, N.W. Kowall, and K. Khrapko. 2006. Mitochondrial DNA deletions are abundant and cause functional impairment in aged human substantia nigra neurons. *Nat. Genet.* 38:518–520. doi:10.1038/ng1778

Le Page, F., E.E. Kwoh, A. Avrutskaya, A. Gentil, S.A. Leadon, A. Sarasin, and P.K. Cooper. 2005. Transcription-coupled repair of 8-oxoguanine: requirement for XPG, TFIIH, and CSB and implications for Cockayne syndrome. *Cell.* 123:711. doi:10.1016/j.cell.2005.11.005

LeDoux, S.P., G.L. Wilson, E.J. Beecham, T. Stevnsner, K. Wassermann, and V.A. Bohr. 1992. Repair of mitochondrial DNA after various types of DNA damage in Chinese hamster ovary cells. *Carcinogenesis.* 13:1967–1973. doi:10.1093/carcin/13.11.1967

Lehmann, A.R. 1995. Nucleotide excision repair and the link with transcription. *Trends Biochem. Sci.* 20:402–405. doi:10.1016/S0968-0004(00)89088-X

Lin, M.T., and M.F. Beal. 2006. Mitochondrial dysfunction and oxidative stress in neurodegenerative diseases. *Nature.* 443:787–795. doi:10.1038/nature05292

Lu, Z., T.W. Fischer, S. Hasse, K. Sugawara, Y. Kamenisch, S. Krengel, W. Funk, M. Berneburg, and R. Paus. 2009. Profiling the response of human hair follicles to ultraviolet radiation. *J. Invest. Dermatol.* 129:1790–1804. doi:10.1038/jid.2008.418

Muftuoglu, M., N.C. de Souza-Pinto, A. Dogan, M. Aamann, T. Stevnsner, I. Rybanska, G. Kirkali, M. Dizdaroglu, and V.A. Bohr. 2009. Cockayne syndrome group B protein stimulates repair of formamido-pyrimidines by NEIL1 DNA glycosylase. *J. Biol. Chem.* 284:9270–9279. doi:10.1074/jbc.M807006200

Nance, M.A., and S.A. Berry. 1992. Cockayne syndrome: review of 140 cases. *Am. J. Med. Genet.* 42:68–84. doi:10.1002/ajmg.1320420115

Nardo, T., R. Oneda, G. Spivak, B. Vaz, L. Mortier, P. Thomas, D. Orioli, V. Laugel, A. Stary, P.C. Hanawalt, et al. 2009. A UV-sensitive syndrome patient with a specific CSA mutation reveals separable roles for CSA in response to UV and oxidative DNA damage. *Proc. Natl. Acad. Sci. USA.* 106:6209–6214. doi:10.1073/pnas.0902113106

Nishioka, K., T. Ohtsubo, H. Oda, T. Fujiwara, D. Kang, K. Sugimachi, and Y. Nakabeppu. 1999. Expression and differential intracellular localization of two major forms of human 8-oxoguanine DNA glycosylase encoded by alternatively spliced OGG1 mRNAs. *Mol. Biol. Cell.* 10:1637–1652.

Osenbroch, P.O., P. Auk-Emblem, R. Halsne, J. Strand, R.J. Forstrøm, I. van der Pluijm, and L. Eide. 2009. Accumulation of mitochondrial DNA damage and bioenergetic dysfunction in CSB defective cells. *FEBS J.* 276:2811–2821. doi:10.1111/j.1742-4658.2009.07004.x

Pang, C.Y., H.C. Lee, J.H. Yang, and Y.H. Wei. 1994. Human skin mitochondrial DNA deletions associated with light exposure. *Arch. Biochem. Biophys.* 312:534–538. doi:10.1006/abbi.1994.1342

Pascucci, B., A. Versteegh, A. van Hoffen, A.A. van Zeeland, L.H. Mullenders, and E. Dogliotti. 1997. DNA repair of UV photoproducts and mutagenesis in human mitochondrial DNA. *J. Mol. Biol.* 273:417–427. doi:10.1006/jmbi.1997.1268

Reinders, J., R.P. Zahedi, N. Pfanner, C. Meisinger, and A. Sickmann. 2006. Toward the complete yeast mitochondrial proteome: multidimensional separation techniques for mitochondrial proteomics. *J. Proteome Res.* 5: 1543–1554. doi:10.1021/pr050477f

Riedl, T., F. Hanaoka, and J.M. Egly. 2003. The comings and goings of nucleotide excision repair factors on damaged DNA. *EMBO J.* 22:5293–5303. doi:10.1093/emboj/cdg489

Riess, T., S.G. Andersson, A. Lupas, M. Schaller, A. Schäfer, P. Kyme, J. Martin, J.H. Wälzlein, U. Ehehalt, H. Lindroos, et al. 2004. Bartonella adhesin a mediates a proangiogenic host cell response. *J. Exp. Med.* 200:1267–1278. doi:10.1084/jem.20040500

Schriner, S.E., N.J. Linford, G.M. Martin, P. Treuting, C.E. Ogburn, M. Emond, P.E. Coskun, W. Ladiges, N. Wolf, H. Van Remmen, et al. 2005. Extension of murine life span by overexpression of catalase targeted to mitochondria. *Science.* 308:1909–1911. doi:10.1126/science.1106653

Stevnsner, T., S. Nyaga, N.C. de Souza-Pinto, G.T. van der Horst, T.G. Gorgels, B.A. Hogue, T. Thorslund, and V.A. Bohr. 2002. Mitochondrial repair of 8-oxoguanine is deficient in Cockayne syndrome group B. *Oncogene.* 21:8675–8682. doi:10.1038/sj.onc.1205994

Stevnsner, T., M. Muftuoglu, M.D. Aamann, and V.A. Bohr. 2008. The role of Cockayne Syndrome group B (CSB) protein in base excision repair and aging. *Mech. Ageing Dev.* 129:441–448. doi:10.1016/j.mad.2008.04.009

Stojanovski, D., N. Pfanner, and N. Wiedemann. 2007. Import of proteins into mitochondria. *Methods Cell Biol.* 80:783–806. doi:10.1016/S0091-679X(06)80036-1

Tanhauser, S.M., and P.J. Laipis. 1995. Multiple deletions are detectable in mitochondrial DNA of aging mice. *J. Biol. Chem.* 270:24769–24775. doi:10.1074/jbc.270.42.24769

Trapp, C., A.K. McCullough, and B. Epe. 2007. The basal levels of 8-oxoG and other oxidative modifications in intact mitochondrial DNA are low even in repair-deficient (Ogg1(−/−)/Csb(−/−)) mice. *Mutat. Res.* 625:155–163.

Trifunovic, A., A. Wredenberg, M. Falkenberg, J.N. Spelbrink, A.T. Rovio, C.E. Bruder, M. Bohlooly-Y, S. Gidlöf, A. Oldfors, R. Wibom, et al. 2004. Premature ageing in mice expressing defective mitochondrial DNA polymerase. *Nature*. 429:417–423. doi:10.1038/nature02517

Tuo, J., M. Müftüoglu, C. Chen, P. Jaruga, R.R. Selzer, R.M. Brosh Jr., H. Rodriguez, M. Dizdaroglu, and V.A. Bohr. 2001. The Cockayne Syndrome group B gene product is involved in general genome base excision repair of 8-hydroxyguanine in DNA. *J. Biol. Chem.* 276:45772–45779. doi:10.1074/jbc.M107888200

van der Horst, G.T., L. Meira, T.G. Gorgels, J. de Wit, S. Velasco-Miguel, J.A. Richardson, Y. Kamp, M.P. Vreeswijk, B. Smit, D. Bootsma, et al. 2002. UVB radiation–induced cancer predisposition in Cockayne syndrome group A (Csa) mutant mice. *DNA Repair (Amst.)*. 1:143–157. doi:10.1016/S1568-7864(01)00010-6

van der Wees, C., J. Jansen, H. Vrieling, A. van der Laarse, A. Van Zeeland, and L. Mullenders. 2007. Nucleotide excision repair in differentiated cells. *Mutat. Res.* 614:16–23.

van Hoffen, A., A.S. Balajee, A.A. van Zeeland, and L.H. Mullenders. 2003. Nucleotide excision repair and its interplay with transcription. *Toxicology*. 193:79–90. doi:10.1016/j.tox.2003.06.001

van Steeg, H., and K.H. Kraemer. 1999. Xeroderma pigmentosum and the role of UV-induced DNA damage in skin cancer. *Mol. Med. Today*. 5:86–94. doi:10.1016/S1357-4310(98)01394-X

Wood, R.D. 1989. Repair of pyrimidine dimer ultraviolet light photoproducts by human cell extracts. *Biochemistry*. 28:8287–8292. doi:10.1021/bi00447a005

Zanna, C., A. Ghelli, A.M. Porcelli, V. Carelli, A. Martinuzzi, and M. Rugolo. 2003. Apoptotic cell death of cybrid cells bearing Leber's hereditary optic neuropathy mutations is caspase independent. *Ann. N.Y. Acad. Sci.* 1010:213–217. doi:10.1196/annals.1299.037